POINTING ACCURACY EVALUATION OF SOTM TERMINALS UNDER REALISTIC CONDITIONS

Mostafa Alazab[1], Wolfgang Felber[2], Giovanni Del Galdo[1], Albert Heuberger[2], Mario Lorenz[2], Markus Mehnert[2], Florian Raschke[2], Gregor Siegert[2], and Markus Landmann*[2]

[1] *Ilmenau University of Technology, Digital Broadcasting Research Lab, Helmholtzplatz 2, 98693 Ilmenau, Germany, name.lastname@tu-ilmenau.de*

[2] *Fraunhofer Institute for Integrated Circuits IIS, Am Wolfsmantel 33, 91058 Erlangen, Germany, name.lastname@iis.fraunhofer.de*

ABSTRACT

The Vehicle-Mounted Earth Stations (VMES) operation requirements defined by the regulatory authorities are bounding for terminal manufacturers. Testing the VMES for these requirements (e.g. pointing accuracy and polarization alignment) is therefore a necessity. The disadvantages of involving operational satellites and having fixed separation between them in traditional test methods are overcome in the proposed test facility. The test facility comprises an antenna tower and a laboratory building. A sensor array is mounted on the antenna tower with the center sensor emulating the satellite. In the laboratory building, the VMES is mounted on a motion emulator which can replay realistic motion profiles. In this contribution, the main components of the test facility are introduced and the performance of the de-pointing measurement system is verified for different VMES motion profiles.

Key words: SOTM, VMES, mobile VSAT, de-pointing measurement, LMS channel, Ka band, Ku band, motion profiles, FCC 25.226, ETSI EN 302977 .

1. INTRODUCTION

The need to access communication services such as the Internet at all times and in all places has become an integral part of our private and professional lives. Especially at places without any terrestrial communication infrastructure, satellite based systems are the only solution. In this context, stationary Very Small Aperture Terminals (VSAT) are already commonly used. During the past years, operators learned that the inaccurate operation of VSAT frequently leads to a degradation of the quality of the offered communication services. A major reason for this degradation is a misalignment of VSAT, i.e., the so called *de-pointing* of the antenna, which has to be avoided in any case to minimize interference to adjacent satellites.

The increasing demand for mobile applications covering land, maritime, and aeronautical environments pushes the development of Vehicle-Mounted Earth Stations (VMES). For these applications, the mobility of the ground terminals represents a significant challenge in complying with the requirements in terms of pointing accuracy. In this context, operators and regulatory authorities are already aware of the need for testing VMES. For instance, in the US the Federal Communications Commission (FCC) [1] and in Europe the European Telecommunications Standards Institute (ETSI) [2] have defined requirements for VMES. These requirements are expressed e.g. in terms of pointing accuracy, required polarization alignment (if non-circular antennas are used), Equivalent Isotropic Radiated Power (EIRP) spectral density limits, and the behavior of the terminal if the satellite signal is lost.

The Fraunhofer Institute for Integrated Circuits IIS in collaboration with Ilmenau University of Technology developed a test facility for Ku/Ka band terminals, which in the following is denoted as the *IIS test facility*. It can realistically and cost efficiently reproduce the operational environment of VMES regardless of the current weather conditions. It allows realistic testing and speeds up the development process of VMES, while lowering the risk of over engineering new systems. This contribution presents evaluation results of a VMES under predefined motion profiles produced at the facility. Based on the results, the compliance with the regulatory requirements is discussed.

In Section 2, the IIS test facility for Ku/Ka band terminals compliant to these requirements is presented. In Section 3, the performance of the de-pointing measurement system is discussed. Section 4 summarizes the main features and outcomes introduced in this

*Contact e-mail: markus.landmann@iis.fraunhofer.de

contribution.

2. THE IIS TEST FACILITY

For system validation and quantitative performance evaluation of VMES, it is desirable to install and operate a test facility which allows for simple, repeatable, and realistic real-time measurements without the need for operational satellites. The Land Mobile Satellite (LMS) channel, the motion of the vehicle and the earth coordinates at which the functionality of the VMES is tested are emulated to reproduce the real world conditions. One could propose to do so in an anechoic chamber, applying a motion emulator and a transmit antenna instead of a satellite. However, for high gain antennas (e.g. dishes with up to 90 cm diameter) this would be prohibitive, as to fulfill the far field condition the required chamber would have to be enormous. In contrast to the latter approach, a tower of 50 m height located 100 m away from the VMES antenna is used to emulate the satellite. In this way, the far field condition can be guaranteed for apertures up to 90 cm diameter. The VMES is mounted on a motion emulator inside an anechoic chamber, having Line of Sight (LoS) through a RF transparent window towards the tower (See Figure 1). In this way, the IIS test facility, as sketched in Figure 2, enables the testing of the overall functionality of the VMES; including antenna elements, Positioning, Acquisition, and Tracking (PAT), and mechanical integration for a satellite elevation of 16° and 24°. In particular, the antenna sub-system can be tested independently both under movement and under the influence of the LMS channel. At this point, the operational environment of a

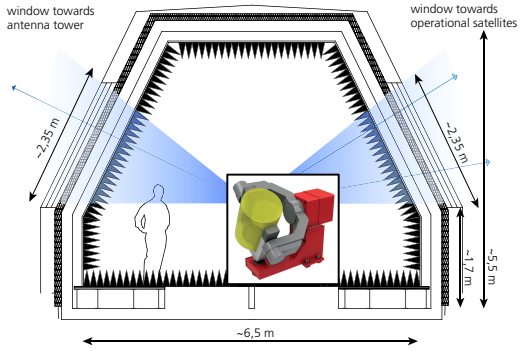

Figure 1. Anechoic chamber with RF transparent windows towards the tower (satellite emulation) and towards operational satellites (45° W to 45° E)

VMES can be reproduced realistically with the IIS test facility.

The IIS test facility comprises the following components (shown in Figure 2):

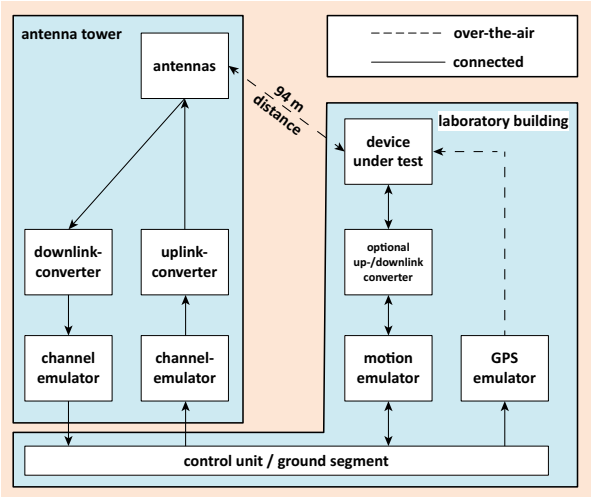

Figure 2. SOTM test bed architecture

- Channel emulators: emulate the fading characteristics caused by the propagation environment; especially blocking/shadowing [3] at Ku/Ka band and weather conditions independently for the uplink and downlink. Channels measured as well as simulated can be employed.
- Motion emulator: emulates mechanical disturbances that act upon a terminal mounted on different types of vehicles (e.g. trucks, cars, ships, etc.) under various conditions (e.g. highways, gravel road, rough sea, etc.). Both generic and measured motion profiles can be applied. For instance, measurements for typical scenarios of emergency aid organizations are available (see also [4] and [5]).
- Navigation emulator: provides arbitrary Global Positioning System (GPS) RF signals for a given set of real latitude and longitude coordinates, which may be necessary for antenna systems utilizing satellite navigation support.
- De-pointing measurement system: a cross shaped sensor array with five antennas is mounted on the antenna tower (see Figure 3). With this fundamental component of the IIS test facility, the de-pointing angle in azimuth and elevation can be accurately determined.

This last component of the IIS test facility is discussed in detail in the following sections. In this context, the performance of the antenna de-pointing measurement system is demonstrated.

3. ANTENNA DE-POINTING MEASUREMENT SYSTEM

To determine the VMES antenna de-pointing, a sensor array as shown in Figure 3 is used. Each box on

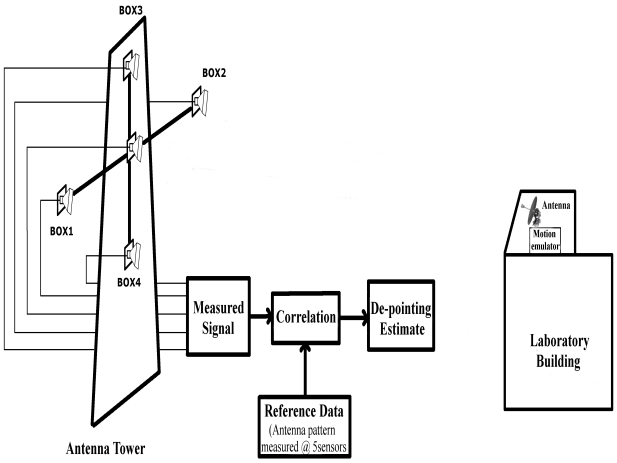

Figure 3. De-pointing measurement setup

the tower contains an antenna for the required frequency (Ku/Ka band) and a power detector. The antenna de-pointing and the sensor positions are defined according to the coordinate system introduced in Figure 4.

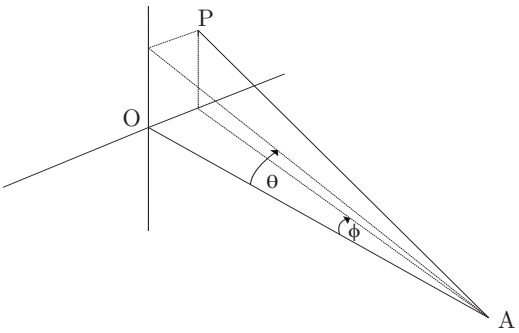

Figure 4. Anetnna de-pointing coordinates. The sensor array is mounted such that the center sensor is located at the origin (point O)

The center sensor is assumed to be at the origin of the coordinate system (point O). The point A represents the position of the antenna and the point P represents the de-pointing direction of the antenna. The angle ϕ is the antenna de-pointing in the horizontal axis while the angle θ is the antenna de-pointing in the vertical axis. The angle notations in Figure 4 are used comprehensively throughout this contribution. The separation between sensors 1 & 2 and between sensors 3 & 4 can be varied in the range $\in [1°, 6°]$, according to the beam-width of the terminal antenna, as explained in detail in Section 3.1.

In a preliminary measurement, the received power at the five sensors is measured for different known antenna de-pointing directions while the tracking system of the antenna is disabled. This data serves as reference for the de-pointing estimation, in which the motion emulator replays a certain motion profile while the tracking system of the antenna is active. At this point, the estimation is carried out in three steps:

1. measure the received signal at the 5 sensors of the VMES
2. calculate the correlation between the measured signal and the reference data
3. the antenna de-pointing estimate results from the maximum of the correlation

3.1. Optimum sensor positions

The de-pointing estimation accuracy is expressed as the standard deviation calculated for a large number of estimation realizations based on Monte Carlo simulations. The optimum sensor positions that yield the best estimation accuracy will be derived in the following. The estimation accuracy depends on three parameters:

- the position of the 4 outer sensors
- the available Signal-to-Noise-Ratio (SNR) at the power detectors
- the 3 dB beam-width of the antenna

The SNR and the 3 dB beam-width of the antenna are fixed parameters since they result from the transmit EIRP of the antenna and the fixed beam of the antenna. Therefore, the positions of the sensors are the only variable parameters that can be adjusted to improve the de-pointing estimation accuracy. In the following, the optimum positions of the sensors are derived for the highest possible de-pointing estimation accuracy w.r.t. the SNR and the 3 dB beam-width of the antenna. Antenna patterns with different 3 dB beam-widths are simulated and the de-pointing estimation accuracy is calculated w.r.t. the positions of the sensors and the SNR. The simulation results lead to an empirical equation for the optimum positions of the sensors with:

$$\Delta \approx (a \cdot \rho^3 + b \cdot \rho^2 + c \cdot \rho + d) \cdot w \qquad (1)$$

where

- Δ is the distance of the outer sensor to the centered sensor along horizontal as well as vertical axes (see Figure 3)
- ρ is the SNR in dB
- w is the 3 dB beam-width of the antenna in degrees
- with the polynomial coefficients $a = -1.3 \cdot 10^{-06}$

- $b = 1.8 \cdot 10^{-04}$
- $c = -7.2 \cdot 10^{-03}$
- $d = 0.709$

Based on Equation (1), the optimum sensor positions w.r.t. the beam-widths and SNR are depicted in Figure 5. The different lines correspond to the

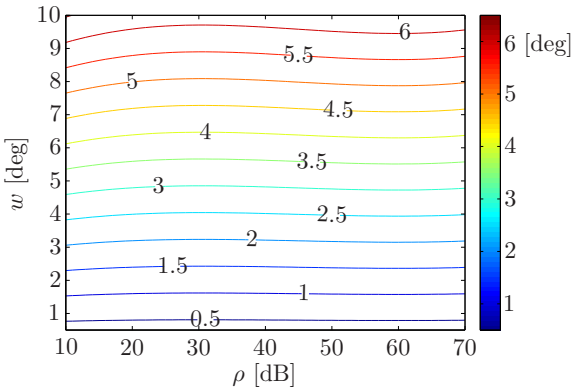

Figure 5. Optimum sensor positions Δ [deg] w.r.t. antenna beam-width and SNR

optimum sensor positions for different beam-widths and SNR values. The maximum achievable estimation accuracy corresponding to the optimum sensor positions are plotted in Figure 6. It can be shown

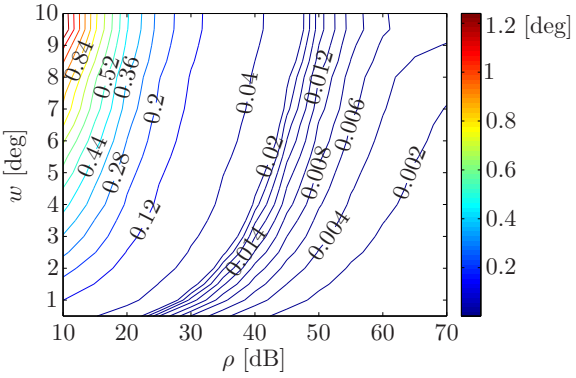

Figure 6. Estimation accuracy for the optimum sensor positions Δ [deg] w.r.t. antenna-beam width and SNR

that at a fixed antenna beam-width, better estimation accuracy can be achieved by increasing the SNR. Assuming that the sensor positions can be adjusted freely, the maximum accuracy as shown in Figure 6 can be achieved. However, the adjustment of the sensors can be very time consuming in practice. If one wanted to test subsequently various terminals with different antenna beam-widths, it would be preferable to keep the sensors at fixed positions for all tests. By defining a minimum de-pointing estimation accuracy (e.g. 0.05°) that has to be achieved in any case, a region w.r.t. sensor position and antenna beam-width can be defined achieving at least the minimum accuracy at a certain SNR. As an example of an estimation accuracy better than 0.05°, these regions are shown in Figure 7 for different SNR values. According to Figure 7, the sensor position can now be chosen in a wider range. For example,

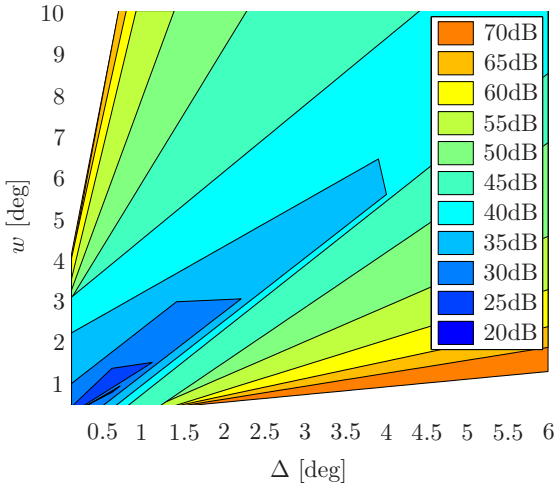

Figure 7. Regions with estimation accuracy better than 0.05°

having an antenna with $w = 5°$ and the sensors fixed at $\Delta = 3°$, the following holds:

- With these sensor positions, the de-pointing estimation accuracy larger than 0.05° can be achieved if the available SNR is not below 35 dB.
- When exchanging the antenna with another antenna having 3 dB beam-width of 4°, we do not need to change the position of the sensors as we can still ensure a minimum accuracy of 0.05° assuming that the SNR is not below 35 dB.
- Ensuring the same accuracy threshold of 0.05° with another antenna having a 3 dB beam-width of 3° requires either:
  - increasing the SNR to be around 10 dB larger (45 dB) while keeping the same sensor positions or,
  - changing the sensor positions to be in the range $\in [1°, 2.3°]$ while keeping the SNR at 35 dB.

3.2. De-pointing Measurement Results

To demonstrate the performance of the de-pointing measurement system, measurements with the following setup were conducted

- High gain antenna as the Device Under Test (DUT) with $w = 1°$
- 5 sensors are included in the measurement as shown in Figure 3
- Sensor positions along vertical and horizontal axes with $\Delta = 1°$
- Ka band (27.5 GHz - 31 GHz)
- Maximum receive SNR between 25 and 35 dB

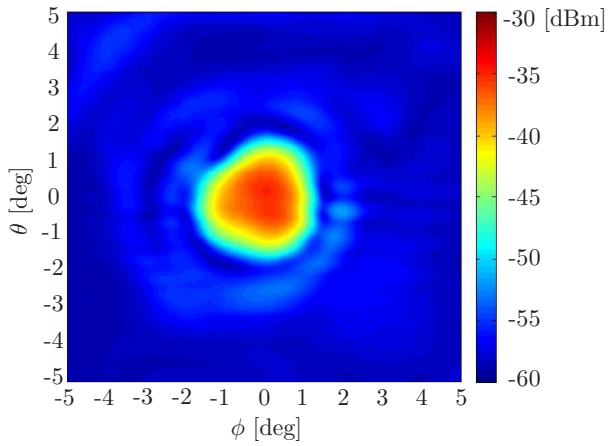

Figure 8. Received power (2D pattern) of the high gain antenna

The received power at the center sensor while rotating the DUT (using the motion emulator) in a 2D (horizontal-vertical) grid is shown in Figure 8. Therefore, the values shown in Figure 8 when properly normalized, may also be interpreted as the directivity function of the high gain antenna.

The performance of the system is analyzed rotating the DUT around the horizontal (one-dimensional) and horizontal&vertical axes (2D) (see Figure 4). The motion profiles are sine functions with a fixed amplitude, frequency and phase. The estimation results for the 1D and 2D case are discussed in the following. During the movement, the DUT tracking mode has been switched off, which means that the estimated de-pointing should exactly correspond to the excitation induced by the motion emulator.

1D de-pointing example: In this example, the antenna moves according to Equation (2)

$$\phi(t) = \alpha_\phi \cdot \sin(2\pi f_\phi t + \psi_\phi) \tag{2}$$

Where the antenna de-pointing follows a time varying sine function along the horizontal axis only with amplitude (α_ϕ), frequency (f_ϕ) and phase (ψ_ϕ). In this example: $\alpha_\phi = 1°$, $f_\phi = 0.1\,\text{Hz}$ and $\psi_\phi = 0°$. The maximum SNR at the power detectors is 35 dB. The terminal antenna is balanced and it can be assumed that there is no play in any of the axes. In Figure 9, the excitation motion profile and the estimation results are depicted. The blue line represents

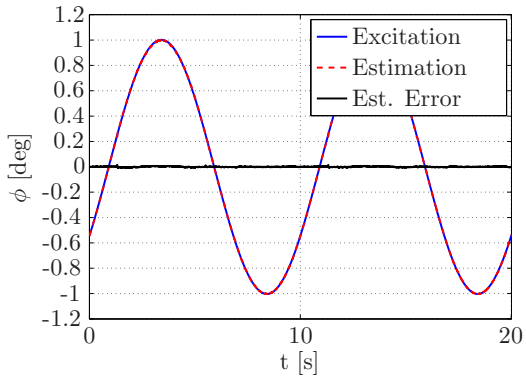

Figure 9. Estimation result for a sine excitation ($f = 1\,\text{Hz}$) along the horizontal axis with $\alpha_\phi = 1°$

the motion excitation, the red dotted line represents the estimation results and the black line represents the estimation error. The Root Mean Square Error (RMSE) and the standard deviation of the estimation results by means of the confidence interval are shown in Figure 10. The RMSE is represented by the blue line and the confidence interval (i.e. standard deviation) is represented using the red bars. The RMSE and the confidence interval are calculated for at least 100 realizations at each de-pointing angle.

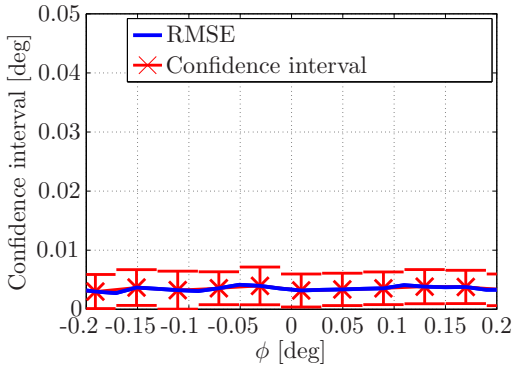

Figure 10. RMSE and confidence interval for a sine excitation ($f = 1\,\text{Hz}$) along the horizontal axis with $\alpha_\phi = 1°$

From Figure 10 it can be seen that the estimation accuracy is in the order of 0.005° on average.

2D de-pointing Example 1: The induced motion along the horizontal and the vertical axes is sinusoidal:

$$\phi(t) = \alpha_\phi \cdot \sin(2\pi f_\phi t + \psi_\phi) \tag{3}$$

and

$$\theta(t) = \alpha_\theta \cdot \sin(2\pi f_\theta t + \psi_\theta) \tag{4}$$

With $\alpha_\phi = \alpha_\theta = 0.5°$, $f_\phi = f_\theta = 0.1\,\text{Hz}$, $\psi_\phi = 0°$ and $\psi_\theta = 90°$. The SNR at the power detectors is around 25 dB. The tracking mode of the terminal antenna is switched off but a small play along the terminals axes can be observed. Furthermore, the antenna itself is not fully weight balanced. The results are shown in a 2D diagram w.r.t. the excitation along the horizontal and vertical axes (Figure 11). The blue circle represents the excitation of the motion emulator while the red dots represents the estimation results.

Analyzing the deviation from the induced excitation, it can be seen that the deviation is smaller than 0.02° on average for both horizontal and vertical axes. This deviation most probably results from the weight imbalance of the terminal antenna and the play along the axes of the terminal.

2D de-pointing Example 2: Again the same settings apply as in the previous example but without phase shift between the two axes in motion i.e. $\psi_\phi = \psi_\theta = 0°$. The results are shown in Figure 12. Again the deviation is smaller than 0.02° on average for both axes and most probably resulting from the weight imbalance and the play along the horizontal and vertical axes.

The results discussed above primarily validate the performance of the IIS test facility and approves its usage for VMES performance testing and validation.

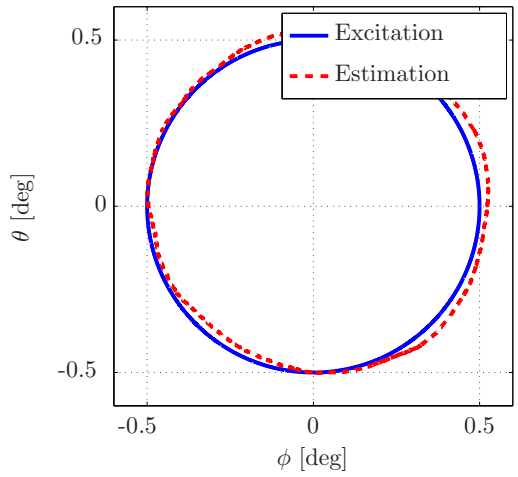

Figure 11. Sine motion excitation for horizontal and vertical axes with phase shift of 90°

4. CONCLUSION

In this contribution the IIS test facility is described. The de-pointing estimation accuracy has been analyzed and evaluated by measurements. The advantages of the IIS test facility and especially the demonstrated de-pointing measurement system compared to system verification with operational satellites can be clearly identified as follows:

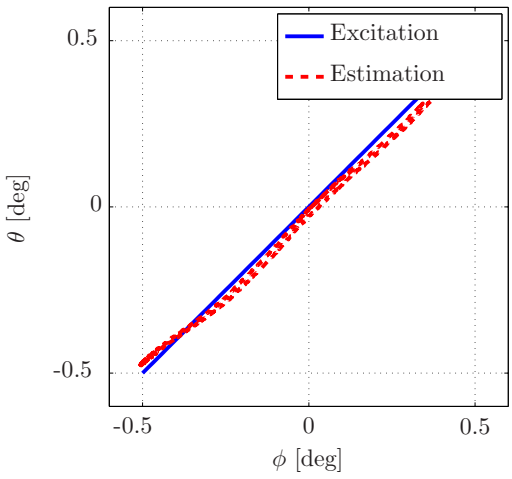

Figure 12. Sine motion excitation for horizontal and vertical axes with phase shift of 0°

- With the proposed sensor array, the de-pointing angle can be determined without involving operational satellites in contrast to satellite to terminal and vice versa measurement.
- The distance between the sensors can be adjusted w.r.t. beam-widths, which results in a higher estimation accuracy of the de-pointing angle.
- De-pointing measurements in azimuth and elevation in contrast to azimuth only are available, which is relevant in case of asymmetric antenna characteristics as in case of low profile antennas.
- Measuring the reference data includes far field radiation pattern measurement (far field condition applies for aperture sizes of up to 90 cm).
- Full communication test of the terminal at Radio Frequency (RF) or Intermediate Frequency (IF).
- Closed loop communication test while changing environment conditions.
- Real operational Geostationary Earth Orbit (GEO) satellites can also be used for testing.
- Comparable conditions for every test run.
- The satellite emulation is available for 16° and 24° elevation.
- Cost-efficient and available at all times.
- Measurements can be carried out regardless of the weather conditions.

Future Extensions: The IIS test facility includes some components and features which are planned to be implemented in the future. The possibility to emulate not only the target satellite but also interfering satellites is planned. Further extensions for polarization de-pointing measurements are to be implemented.

REFERENCES

[1] FCC. FCC 25.226; Blanket licensing provisions for domestic, U.S. Vehicle-Mounted Earth Stations (VMES), 2010.

[2] ETSI EN 302 977 V 1.1.2, Satellite Earth Stations and Systems (SES); Harmonized EN for Vehicle-Mounted Earth Stations (VMES) operating in the 14/12 GHz frequency bands covering essential requirements under article 3.2 of the R&TTE directive, 2010.

[3] Marie Rieche, Daniel Arndt, Alexander Ihlow, Markus Landmann, and Giovanni Del Galdo. Image-based state modeling of the land mobile satellite channel for multi-satellite reception. In *34rd ESA Antenna Workshop on Challenges for Space Antenna Systems*, ESTEC, Noordwijk, Niederlande, October 2012. ESA. zur Veröffentlichung angenommen.

[4] ESA Project ARTES-5.1 - 7-.022 - AO-6669: Mobile Tracking Needs Website under: http://telecom.esa.int/telecom/.

[5] Lorenz M., Mehnert M., and Heuberger A. Measurements of mechanical disturbances of vehicle mounted, mobile very small aperture terminals (vsat). In *Proceedings of the 11th Workshop Digital Broadcasting*, pages 61–65, Erlangen, Germany, September 2010.